Artificial Metalloenzymes

DOI: 10.1002/anie.200704865

X-Ray Structure and Designed Evolution of an Artificial Transfer Hydrogenase**

Marc Creus, Anca Pordea, Thibaud Rossel, Alessia Sardo, Christophe Letondor, Anita Ivanova, Isolde LeTrong, Ronald E. Stenkamp, and Thomas R. Ward**

While the optimization of enzyme performance is a well-established and active field of research, the creation of activity out of nothing within an existing protein scaffold remains a daunting task.[1–3] To overcome this challenge, a catalytically active organometallic moiety anchored within a protein scaffold represents an attractive starting point for both chemical and genetic optimization of the resulting artificial metalloenzyme.[4–9] Guided by the structure of an artificial transfer hydrogenase based on biotin–streptavidin technology, we have implemented a designed evolution protocol to identify both *R*- and *S*-selective variants for reduction of acetophenone derivatives (up to 96% *ee*) as well as dialkyl ketone substrates (up to 90% *ee*).

An early report by Wilson and Whitesides[10] inspired the use the biotin–streptavidin technology to produce artificial hydrogenases for the enantioselective reduction of nitrogen-protected dehydroamino acids[11–14] as well as for the reduction of acetophenone derivatives by transfer hydrogenation.[15,16] Previous studies on artificial transfer hydrogenases have allowed the identification of promising systems for the reduction of acetophenone derivatives: [η^6-(benzene)RuCl(Biot-*p*-L)]⊂S112K Sav (Sav = streptavidin, Biotin-*p*-L = *N*′-(4-Biotinamidophenylsulfonyl)ethylenediamine; see Figure 2) and [η^6-(*p*-cymene)RuCl(Biot-*p*-L)]⊂S112A Sav afford (*S*)- and (*R*)-phenylethanol reduction products, respectively.[15,16] Alternative anchoring strategies have been exploited to afford artificial metalloenzymes for ester hydrolysis,[17] dihydroxylation,[18] sulfoxidation,[19,20] epoxidation,[21,22] and Diels–Alder reactions.[23–25]

The mechanism of the transfer hydrogenation of aromatic ketones using piano-stool complexes incorporating amino-sulfonamide ligands is well-established. The enantiodiscrimination event relies on C–H···π interactions between the substrate and the η^6-bound arene.[26] Within this context, the reduction of dialkyl ketones remains challenging.[27] Nature relies mostly on NAD(P)H-containing enzymes for such reactions, with the entire second coordination sphere of the active site in alcohol dehydrogenases being tailored for such tasks.[28,29]

In recent years, there has been an increasing effort to combine rational design features into Darwinian evolutionary protocols.[30–34] Designed evolution combines rational decisions on sites of mutations with rounds of screening to perfect those elements of enzyme function that cannot be predicted. With this aim, [η^6-(benzene)RuCl(Biot-*p*-L)]⊂S112K Sav was crystallized, and its X-ray structure is displayed in Figure 1 (PBD reference code 2QCB). Structural details are collected in the Supporting Information. In the refined model (1.58-Å resolution, $R = 0.168$, $R_{free} = 0.187$), several relevant features are identified:

1) The piano-stool moiety and the S112K side chain are only partially occupied (20% and 50%, respectively, Figure 1a). This finding may be traced back to a) conformational flexibility of the piano-stool moiety within the host protein, b) ruthenium decomplexation during cocrystallization in the presence of 1.0 M sodium citrate, or c) a short contact with a neighboring biotinylated complex (Ru···Ru separation 4.44 Å) within the streptavidin tetramer that hinders the occupancy of the adjacent biotin binding site in this ordered conformation.
2) Short contacts between the Ru complex and amino acids in several loop regions can be identified (Figure 1b).
3) Incorporation of the bulky biotinylated complex [η^6-(benzene)RuCl(Biot-*p*-L)] within S112K Sav does not lead to a major structural reorganization of the host protein. Compared to wild-type (WT) Sav (PDB reference code 1STP), a root mean square (RMS) of 0.276 Å is computed for all 121 C_α atoms present (Figure 1c).
4) Despite the use of a "racemic" piano-stool complex for crystallization, the configuration at ruthenium is *S* in the crystal structure (Figure 1b). Most interestingly, the (*S*)-Ru configuration in a homogeneous system leads to (*S*)-phenylethanol reduction products,[26] corresponding to the preferred enantiomer produced with [η^6-(benzene)RuCl(Biot-*p*-L)]⊂S112K Sav.[15]

[*] Dr. I. LeTrong, Prof. R. E. Stenkamp[++]
Departments of Biological Structure and Biochemistry and the Biomolecular Structure Center, University of Washington
Box 357420 Seattle, WA 98195-7420 (USA)
Fax: (+1) 206-543-1524
E-mail: stenkamp@u.washington.edu
Dr. M. Creus,[+] A. Pordea,[+] T. Rossel, A. Sardo, Dr. C. Letondor, Dr. A. Ivanova, Prof. T. R. Ward[++]
Institute of Chemistry, University of Neuchâtel
Av. Bellevaux 51, CP 158, 2009 Neuchâtel (Switzerland)
Fax: (+41) 32-718-2511
E-mail: thomas.ward@unine.ch
[+] These authors contributed equally to this work.
[++] Corresponding authors: Prof. Stenkamp for the X-ray structure, Prof. Ward for all other matters.

[**] This work was funded by the Swiss National Science Foundation (Grants FN 200021-105192 and 200020-113348), the Roche Foundation as well as the FP6 Marie Curie Research Training network (MRTN-CT-2003-505020) and the Canton of Neuchâtel. We thank Umicore Precious Metals Chemistry for a loan of ruthenium. We thank C. R. Cantor for the streptavidin gene.

Supporting information for this article is available on the WWW under http://www.angewandte.org or from the author.

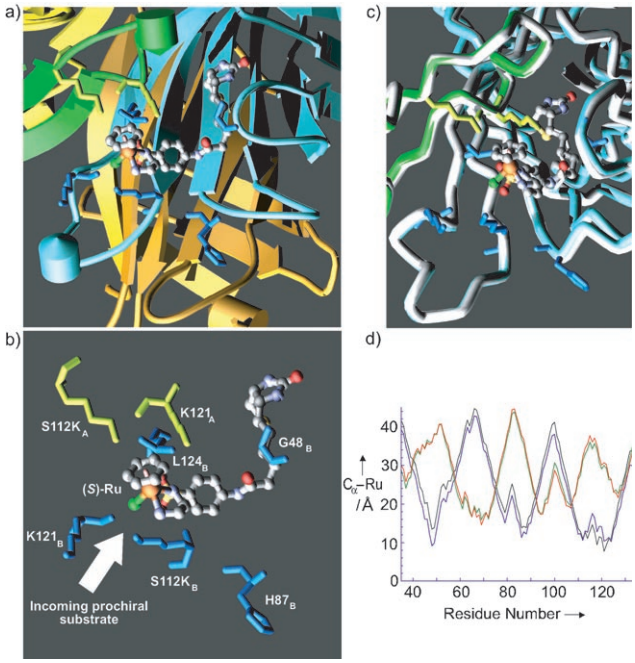

Figure 1. X-ray crystal structure of [η^6-(benzene)RuCl(Biot-*p*-L)]⊂S112K Sav. a) Close-up view (only monomer B (blue) occupied by the biotinylated catalyst (ball-and-stick representation); monomers A (green), C (orange), and D (yellow)). b) Highlight of amino acid side-chain residues displaying short contacts with Ru. The absolute configuration at ruthenium is *S*. c) Superimposition of the structure of [η^6-(benzene)RuCl(Biot-*p*-L)]⊂S112K Sav with the structure of biotin⊂core streptavidin (PDB reference code 1STP, only monomers A and B displayed for clarity; biotin: white stick, core streptavidin: white tube). d) Ru–C_α distances extracted from the X-ray structure of [η^6-(benzene)RuCl(Biot-*p*-L)]⊂S112K Sav; monomers: A black, B blue, C green, and D red.

5) Substituting the capping η^6-benzene ligand with the bulkier η^6-*p*-cymene may force the latter biotinylated complex to adopt a different position or configuration at the metal center to avoid steric clash between the η^6-arene and the amino acid residues $112K_A$ and $121K_A$.

On the basis of this structure, we selected positions K121 and L124 for saturation mutagenesis, using the genetic backgrounds of WT Sav, S112A Sav, or S112K Sav to afford a total of 117 Sav isoforms (See the Supporting Information). Position K121 was of particular interest, as both $K121_A$ and $K121_B$ residues (A and B refer to the respective monomers; see Figure 1) may interact both with the η^6-arene (i.e. $K121_A$) and with the incoming substrate (i.e. $K121_B$). We targeted residue L124, as we speculated that saturation mutagenesis at this position may subtly alter the position of the biotinylated catalyst ($H_3C_{Leu}\cdots OSORR_{Ligand}$ 3.53 Å).

To accelerate the optimization process, a straightforward extraction–immobilization protocol with biotin–sepharose was implemented to capture functional Sav from crude cellular extracts.[14] Indeed, we hypothesized that, owing to the high affinity of biotin for streptavidin, one biotin-binding site could be used for immobilization, leaving up to three binding sites to accommodate the biotinylated catalyst.

Each of the immobilized isoforms was combined with either [η^6-(benzene)RuCl(Biot-*p*-L)] or [η^6-(cymene)RuCl-(Biot-*p*-L)] and tested for the reduction of ketones **1** and **3** (Scheme 1). Although the purification and immobilization

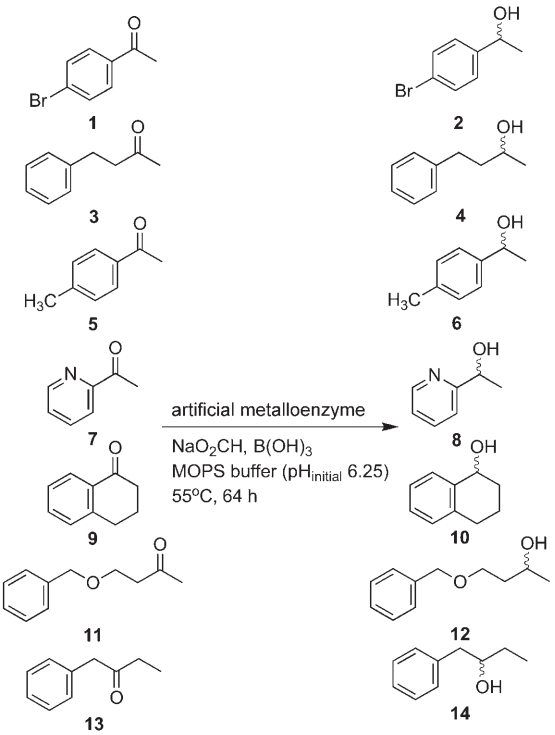

Scheme 1. Substrates, reduction products, and operating conditions used for the designed evolution of artificial transfer hydrogenases. η^6-arene = benzene, *p*-cymene; Sav mutant: K121X, L124X, S112A K121X, S112K K121X, S112A L124X, S112K K124X. The catalytic runs were performed at 55 °C for 64 h using the mixed buffer NaO_2CH (0.48 M), $B(OH)_3$ (0.41 M), and 3-(*N*-morpholino)propanesulfonic acid (MOPS, 0.16 M) at $pH_{initial}$ 6.25. Ru/substrate/formate ratio 1:100:4000

with biotin–sepharose led to an erosion of both the activity and the selectivity (Table 1), this protocol significantly hastened the screening process to identify trends. The results obtained with the immobilized artificial metalloenzymes are summarized in the form of a fingerprint (Figure 2). The most promising results were reproduced using the purified non-immobilized catalyst in the presence of representative substrates (Scheme 1 and Table 1, see the Supporting Information for a comprehensive list of all catalytic runs).

On the basis of this screening, several interesting features can be identified:

1) Irrespective of the substrate, the nature of the η^6-arene plays an important role in determining the preferred enantiomer (Figure 2).[15,16] Strikingly, substitution of η^6-benzene for η^6-*p*-cymene in the presence of S112A K121N Sav affords near mirror images for the reduction of both substrates **1** and **3** (Table 1 entries 4–7).
2) Both substrates **1** and **3** behave similarly in terms of selectivity (Table 1 and Figure 3b). While the enantioselectivity for the reduction of aryl ketone derivatives can be

Table 1: Summary of selected results for the catalytic experiments with either biotin–sepharose immobilized or purified homogeneous artificial metalloenzymes [η^6-(arene)RuH(Biot-*p*-L)]⊂Sav.

Entry	Arene	Sav isoform	Ketone	*ee* (conv [%]) extract[a,b]	*ee* (conv [%]) pure[a,c]
1	*p*-cymene	WT Sav	**1**	65 (81)	87 (93)
2	benzene	WT Sav	**1**	−39 (31)	−57 (43)
3	*p*-cymene	L124V	**1**	83 (90)	91 (96)
4	benzene	S112A K121N	**1**	−55 (99)	−75 (98)
5	*p*-cymene	S112A K121N	**1**	50 (63)	70 (89)
6	benzene	S112A K121N	**3**	−62 (95)	−72 (quant.)
7	*p*-cymene	S112 A K121N	**3**	58 (81)	70 (78)
8	benzene	S112K L124H	**1**	−59 (64)	−65 (94)
9	*p*-cymene	S112A K121T	**3**	82 (84)	88 (99)
10	benzene	K121R	**1**	−64 (96)	−68 (95)
11	*p*-cymene	S112A K121S	**3**	59 (80)	77 (98)
12	benzene	S112A K121W	**3**	80 (86)	84 (99)
13	*p*-cymene	L124V	**5**	–	96 (97)
14	benzene	S112A K121N	**7**	–	−92 (quant.)
15	*p*-cymene	S112A K121T	**11**	–	90 (quant.)
16	*p*-cymene	L124V	**9**	–	87 (20)
17	benzene	S112A K121N	**9**	–	−92 (54)
18	*p*-cymene	S112A K121T	**13**	–	46 (50)

[a] Positive and negative *ee* values correspond to the *R* and *S* enantiomers, respectively. [b] Immobilized protein from crude cellular extract. [c] Purified non-immobilized protein. – = not performed.

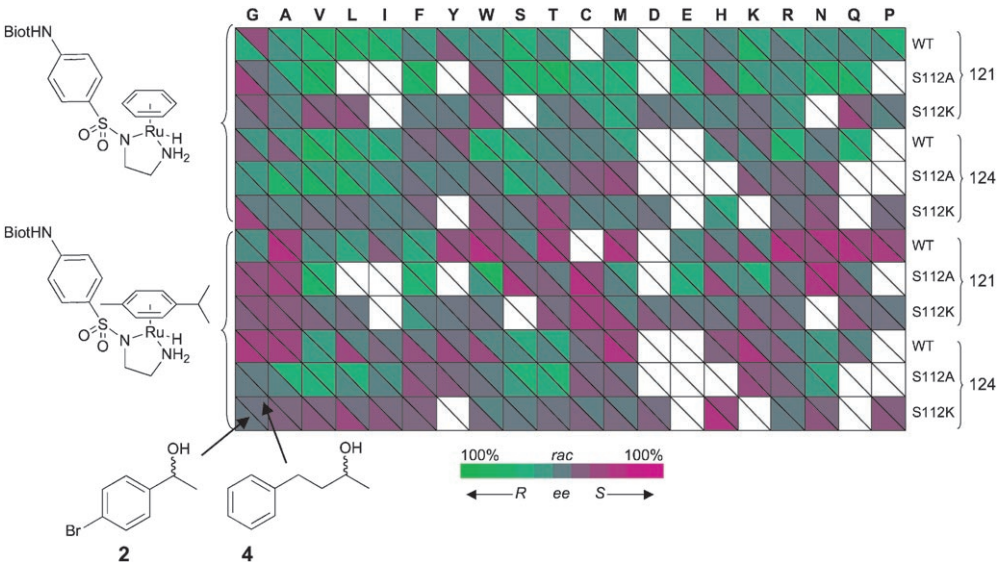

Figure 2. Fingerprint display of the results for the chemogenetic optimization of the reduction of ketones **1** and **3** in the presence of biotin–sepharose-immobilized artificial metalloenzymes [η^6-(arene)RuH(Biot-*p*-L)]⊂Sav mutant. Catalytic runs which could not be performed (insufficient soluble protein expression, see the Supporting Information) are represented by white triangles.

optimized to levels of greater than 90% *ee* with Sav isoforms bearing a single point mutation,[15,16] a designed evolution protocol was required to identify Sav double mutants that afford dialkyl reduction products in up to 90% *ee*.

3) Artificial metalloenzymes incorporating the S112A mutation give better enantioselectivities than the systems bearing the S112K mutation (Figure 3c). A small side chain at position S112 may allow increased influence of beneficial K121X or L124X mutations.
4) Overall, saturation mutagenesis at position K121 is more effective for the optimization of enantioselectivity than saturation mutagenesis at position L124 (Figure 3d). We speculate that this effect may be due to the influence of the K121X side chains both on the piano-stool complex itself ($K121X_A$) and on the trajectory of the incoming prochiral substrate ($K121X_B$; Figure 1b). This latter interaction may be particularly important for the challenging dialkyl ketone substrates **3** and **11**, as it provides a second-coordination-sphere interaction with the substrate, reminiscent of natural enzymes.
5) Methyl alkyl and methyl aryl ketones afford good levels of conversion and selectivity (up to 96% *ee* (*R*) for **6**, 92% *ee* (*S*) for **8**, and 90% *ee* (*R*) for **12**; Table 1, entries 13–15). In contrast, ketones bearing a longer alkyl group give comparatively modest conversions (Table 1, entries 16–18), suggesting that such artificial metalloenzymes may be further evolved to display high substrate specificity. Such substrate specificity is similar to yeast alcohol dehydrogenase which in general only accepts aldehydes and methyl ketones as substrates.[29]

In summary, the structural characterization of [η^6-(benzene)RuCl(Biot-*p*-L)]⊂S112K Sav has allowed us to implement a designed evolution protocol for the optimization of artificial transfer hydrogenases. A straightforward immobilization step using biotin–sepharose, performed on crude cellular extracts, allowed the identification of [η^6-(*p*-cymene)RuH(Biot-*p*-L)]⊂S112A K121T Sav for the enantioselective reduction of dialkyl ketones (up to 90% *ee* for **12;** Table 1, entry 15). This artificial metalloenzyme is attained by an evolutionary path involving a combination of two poorly adapted mutations that would not normally be selected individually (Figure 3e). Interaction between the host protein and the substrate clearly contributes to enantioselectivity. This notion is consistent with the evolution of artificial transfer hydrogenases for dialkyl ketones, which cannot rely on a C–H···π interaction as an enantiodiscriminating element. Thus, screening for enantioselectivity likely optimizes interactions between substrate and the second coordination sphere provided by the protein, exerting a strong evolutionary pressure toward substrate

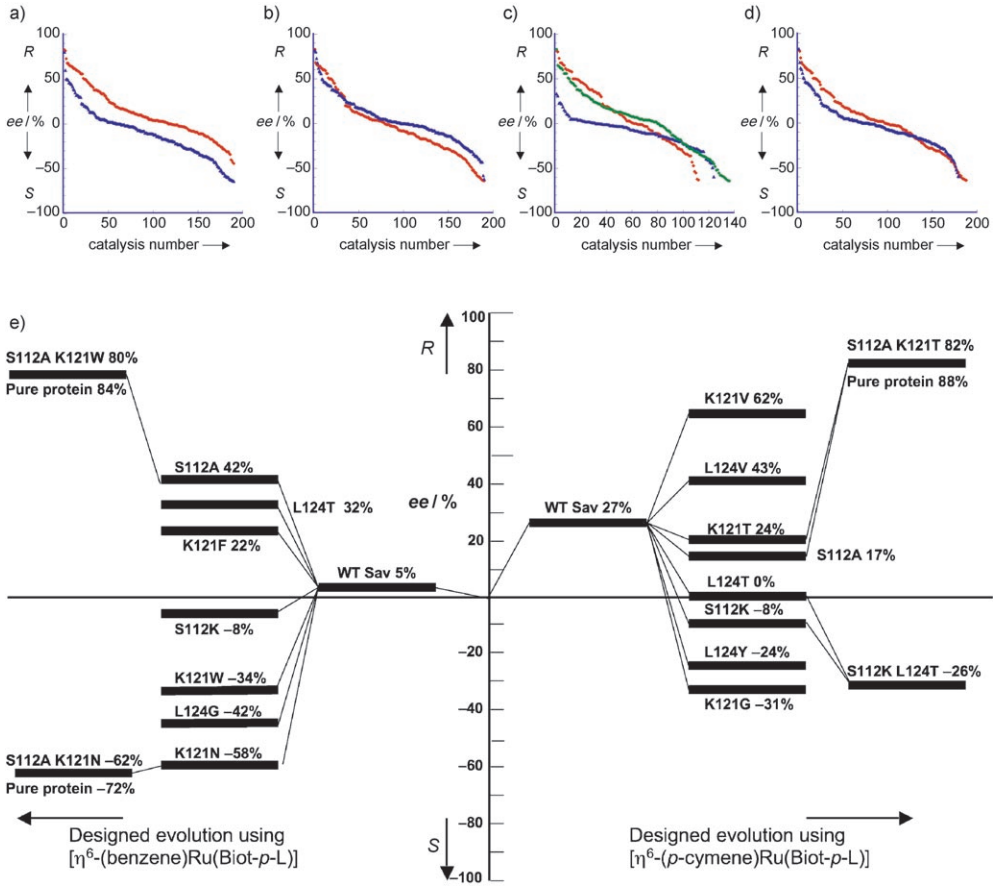

Figure 3. Enantioselectivity trends of artificial transfer hydrogenases. Graphical summary for the immobilized protein arranged according to: a) The nature of the capping η^6-arene: benzene (▲) and *p*-cymene (◆). b) The nature of the products **2** (◆) or **4** (▲). c) The nature of the S112X residue: S112A (◆), S112K (▲), S112 (●). d) The position of the site of mutation: K121X (◆) or L124X (▲). e) Reconstructed evolutionary path of the best *R*- and *S*-selective hybrid catalysts for the reduction of 4-phenyl-2-butanone **3**. Only the best single mutations and those present in the best double mutants are listed.

specialization. Such specialized artificial enzymes, obtainable by designed evolution with modest screening efforts, hold great potential for applications in both white and red biotechnology.

Received: October 19, 2007
Published online: January 4, 2008

Keywords: asymmetric catalysis · chemogenetic optimization · directed evolution · hydrogenation · metalloenzymes

[1] M. A. Dwyer, L. L. Looger, H. W. Hellinga, *Science* **2004**, *304*, 1967.
[2] H.-S. Park, S.-H. Nam, J. K. Lee, C. N. Yoon, B. Mannervik, S. J. Benkovic, H.-S. Kim, *Science* **2006**, *311*, 535.
[3] B. Seelig, J. W. Szostak, *Nature* **2007**, *448*, 828.
[4] D. Qi, C.-M. Tann, D. Haring, M. D. Distefano, *Chem. Rev.* **2001**, *101*, 3081.
[5] C. M. Thomas, T. R. Ward, *Chem. Soc. Rev.* **2005**, *34*, 337.
[6] C. Letondor, T. R. Ward, *ChemBioChem* **2006**, *7*, 1845.
[7] Y. Lu, *Angew. Chem.* **2006**, *118*, 5714; *Angew. Chem. Int. Ed.* **2006**, *45*, 5588.
[8] T. Ueno, T. Koshiyama, S. Abe, N. Yokoi, M. Ohashi, H. Nakajima, Y. Watanabe, *J. Organomet. Chem.* **2007**, *692*, 142.
[9] M. Breuer, K. Ditrich, T. Habicher, B. Hauer, M. Kesseler, R. Stürmer, T. Zelinski, *Angew. Chem.* **2004**, *116*, 806; *Angew. Chem. Int. Ed.* **2004**, *43*, 788.
[10] M. E. Wilson, G. M. Whitesides, *J. Am. Chem. Soc.* **1978**, *100*, 306.
[11] C.-C. Lin, C.-W. Lin, A. S. C. Chan, *Tetrahedron: Asymmetry* **1999**, *10*, 1887.
[12] G. Klein, N. Humbert, J. Gradinaru, A. Ivanova, F. Gilardoni, U. E. Rusbandi, T. R. Ward, *Angew. Chem.* **2005**, *117*, 7942; *Angew. Chem. Int. Ed.* **2005**, *44*, 7764.
[13] M. T. Reetz, J. J.-P. Peyeralans, A. Maichele, Y. Fu, M. Maywald, *Chem. Commun.* **2006**, 4318.
[14] U. E. Rusbandi, C. Lo, M. Skander, A. Ivanova, M. Creus, N. Humbert, T. R. Ward, *Adv. Synth. Catal.* **2007**, *349*, 1923.
[15] C. Letondor, N. Humbert, T. R. Ward, *Proc. Natl. Acad. Sci. USA* **2005**, *102*, 4683.
[16] C. Letondor, A. Pordea, N. Humbert, A. Ivanova, S. Mazurek, M. Novic, T. R. Ward, *J. Am. Chem. Soc.* **2006**, *128*, 8320.
[17] R. R. Davies, M. D. Distefano, *J. Am. Chem. Soc.* **1997**, *119*, 11643.
[18] T. Kokubo, T. Sugimoto, T. Uchida, S. Tanimoto, M. Okano, *J. Chem. Soc. Chem. Commun.* **1983**, 769.
[19] F. van de Velde, L. Könemann, F. van Rantwijk, R. A. Sheldon, *Chem. Commun.* **1998**, 1891.
[20] A. Mahammed, Z. Gross, *J. Am. Chem. Soc.* **2005**, *127*, 2883.
[21] K. Okrasa, R. J. Kazlauskas, *Chem. Eur. J.* **2006**, *12*, 1587.

[22] A. Fernandez-Gacio, A. Codina, J. Fastrez, O. Riant, P. Soumillon, *ChemBioChem* **2006**, *7*, 1013.
[23] G. Roelfes, B. L. Feringa, *Angew. Chem.* **2005**, *117*, 3294; *Angew. Chem. Int. Ed.* **2005**, *44*, 3230.
[24] M. T. Reetz, N. Jiao, *Angew. Chem.* **2006**, *118*, 2476; *Angew. Chem. Int. Ed.* **2006**, *45*, 2416.
[25] G. Roelfes, A. J. Boersma, B. L. Feringa, *Chem. Commun.* **2006**, 635.
[26] M. Yamakawa, I. Yamada, R. Noyori, *Angew. Chem.* **2001**, *113*, 2900; *Angew. Chem. Int. Ed.* **2001**, *40*, 2818.
[27] A. Schlatter, M. K. Kundu, W.-D. Woggon, *Angew. Chem.* **2004**, *116*, 6899; *Angew. Chem. Int. Ed.* **2004**, *43*, 6731.
[28] L. A. LeBrun, D.-H. Park, S. Rmaswamy, B. W. Plapp, *Biochemistry* **2004**, *43*, 3014.
[29] K. Faber, *Biotransformations in Organic Chemistry*, 5th ed., Springer, Berlin, **2004**.
[30] A. Schmid, J. S. Dordick, B. Hauer, A. Kiener, M. Wubbolts, B. Witholt, *Nature* **2001**, *409*, 258.
[31] H. E. Schoemaker, D. Mink, M. G. Wubbolts, *Science* **2003**, *299*, 1694.
[32] C. A. Voigt, S. L. Mayo, F. H. Arnold, Z.-G. Wang, *Proc. Natl. Acad. Sci. USA* **2001**, *98*, 3778.
[33] M. T. Reetz, M. Bocola, J. D. Carballeira, D. Zha, A. Vogel, *Angew. Chem.* **2005**, *117*, 4264; *Angew. Chem. Int. Ed.* **2005**, *44*, 4192.
[34] M. T. Reetz, *Nat. Protoc.* **2007**, *2*, 891.

